Steel and Composite Structures, *Vol. 32, No. 2 (2019) 239-252*
DOI: https://doi.org/10.12989/scs.2019.32.2.239

Vibration analysis of sandwich truncated conical shells with porous FG face sheets in various thermal surroundings

Mohsen Rahmani [1b], Younes Mohammadi [*1] and Farshad Kakavand [2a]

[1] *Faculty of Industrial and Mechanical Engineering, Qazvin Branch, Islamic Azad University, Qazvin, Islamic Republic of Iran*
[2] *Department of Mechanical Engineering, Takestan Branch, Islamic Azad University, Takestan, Islamic Republic of Iran*

(*Received February 22, 2019, Revised April 27, 2019, Accepted June 4, 2019*)

Abstract. Since conical sandwich shells are important structures in the modern industries, in this paper, for the first time, vibration behavior of the truncated conical sandwich shells which include temperature dependent porous FG face sheets and temperature dependent homogeneous core in various thermal conditions are investigated. A high order theory of sandwich shells which modified by considering the flexibility of the core and nonlinear von Karman strains are utilized. Power law rule which modified by considering the two types of porosity volume fractions are applied to model the functionally graded materials. By utilizing the Hamilton's energy principle, and considering the in-plane and thermal stresses in the face-sheets and the core, the governing equations are obtained. A Galerkin procedure is used to solve the equations in a simply supported boundary condition. Uniform, linear and nonlinear temperature distributions are used to model the effect of the temperature changing in the sandwich shell. To verify the results of this study, they are compared with FEM results obtained by Abaqus software and for special cases with the results in literatures. Eigen frequencies variations are surveyed versus the temperature changing, geometrical effects, porosity, and some others in the numerical examples.

Keywords: free vibration; truncated conical sandwich shell; FGM; temperature-dependent; porosity

1. Introduction

After the first considering sandwich constructions in research paper in 1944, these modern structures with high flexural stiffness to weight ratio have become a favorite structures among the researchers. Sandwiches include two faces to resist the in-plane and bending loads and a core to resist the transverse shear loads and maintain the faces distance (Vinson 2018).

Due to interlayer jointing problems, failure, delamination and thermal stress concentration in high temperature environments, application of usual materials and ordinary composites is not proper. Japanese researchers proposed functionally graded materials to overcome these problems. FGMs are microscopic inhomogeneous materials which gradually graded from a metal surface to a ceramic one (Mahamood and Akinlabi 2017). Investigation on these materials have been increased by material researchers. Chen *et al*. (2017) by applying the FGM in the faces of the sandwich plates studied the vibration and buckling behavior in the thermal condition. A power law rule was considered to model the material properties. Benlahcen *et al*. (2018) by using FGM in the plates studied the buckling behavior of these structures in a simply supported condition. Khayat *et al*. (2018) investigated the free vibration of FG cylindrical shells. The material properties of FGM varied gradually in thickness direction in accordant to power law rule. Bouderba (2018) studied the bending of FGM rectangular plates in thermal condition. Properties varied in thickness direction based on a power law rule.

During the production process of FGMs, some micro voids appear which affect the material properties. Considering porosity in the modeling of these materials is a development in the researches. Atmane *et al*. (2015) investigated the free vibration of porous FG beams by considering porosity phases. Boutahar and Benamar (2016) investigated the vibration behavior of porous FG annular plates with elastic foundations. They modified the mixture rule by considering the porosity volume fraction in the FGM. Benferhat *et al*. (2016) studied the static behavior of porous FG plates. Since micro voids appear in FG material, they modified the power law rule by considering porosity. Akbas (2017) investigated the post-buckling behavior of porous FG beams. The power law rule was modified by considering different types of porosity. Wang and Zu (2017) surveyed the vibration of the porous FG rectangular plates in different thermal conditions. Defects in production process causes to consider two types of porosity distribution, namely, even and uneven.

There are several approaches to investigate the mechanical behavior of sandwich structures such as finite element model, shear deformation theories, 3D elastic theory and energy methods (Reddy 2000). Barka *et al*. (2016) studied the post-buckling behavior of FG faces sandwich plates resting on elastic foundation by using a shear deformation theory. Shokravi (2017) by applying Reddy shear deformation theory studied the buckling of FG sandwich plates resting on elastic medium. Tahouneh

*Corresponding author, Ph.D., Assistant Professor,
E-mail: u.mohammadi@gmail.com

ISSN: 1229-9367 (Print), 1598-6233 (Online)

(2018) investigated the vibration behavior of sandwich sectorial plates by using a 3D elasticity theory. Reddy (2007) collected a summary of these methods. In these theories the height of the core is constant, but in fact the thickness of the sandwich plates is variable. So, the core layer should be considered as the flexible layer that compressed transversely. In the classical theories, the localized effects in the core can't be calculated, so to consider these effects, Frostig *et al*. (1992) presented a high order theory. Liu *et al*. (2015) studied the free vibration of the FG sandwich plates by applying a high order theory. Fard (2015) by applying a high order sandwich panel theory studied the static behavior of conical composite sandwich panel. Frostig *et al*. (2018) surveyed the wrinkling of FG sandwich panels by using the extended high order theory. Salami and Dariushi (2018) by using a high order theory surveyed the low velocity impact response of composite sandwich beam.

Considering the dependency of material properties to the temperature, and distribution of the temperature in the thickness direction of the structure are important to model the mechanical behavior of the sandwich panels. A review in literature shows there are limited researches that consider temperature dependent materials for both faces and core concurrently. Khalili and Mohammadi (2012) by applying a high order theory studied the free vibration of FG rectangular sandwich plates with temperature dependent materials. They assumed a uniform temperature distribution in the thickness direction. Dehkordi and Khalili (2015) studied the frequencies of SMA sandwich plates by applying a finite element model. They assumed temperature dependent material for the core. Arioui *et al.* (2018) studied the thermal buckling of temperature dependent FGM beams by using a beam theory. Kettaf *et al*. (2013) by using a shear deformation model studied the buckling of FG plates under uniform, linear and nonlinear temperature rises. Fazzolari (2015) investigated the free vibration and thermal stability of FG sandwich plates by using a Ritz method. He considered the uniform, linear and nonlinear temperature distribution in the thickness direction. Menasria *et al*. (2017) investigated the thermal stability of FG sandwich plates. They assumed thermal load as uniform, linear and nonlinear temperature distributions along the thickness. Talebitooti (2018) investigated the effects of thermal load on the vibration of a rotating FG conical shell. Temperature is distributed nonlinearly within the thickness direction.

Conical sandwich shells are important kinds of structural components which have been applied in advanced industries such as aerospace, mechanical and nuclear engineering. By using FGMs which have high thermal strength within the conical shells, application of these structures significantly have been increased. Despite the importance of these modern structures, due to the complex set of partial differential equations, there are little literature about conical sandwich shells comparing with cylindrical shells and circular plates (Jin *et al*. 2015, Sofiyev 2016). Recently, FG truncated conical shells have been applied in military aircraft propulsion system, missile bodies, pressure vessels, oil tanks, nuclear reactors, rockets, water ducts, pipelines and casing pipes, process equipment, fuselage structures in the region of the exhaust ducts/propeller plane and rotary dryers (Sofiyev 2015, Van Dung and Chan 2017, Sofiyev and Kuruoglu 2015, Sofiyev and Schnack 2012, Malekzadeh *et al*. 2012, Bardell *et al*. 1999, Talebitooti 2018).

So, it is important to investigate the vibration behavior of the conical sandwich shells with FG face sheets. Liu and Li (1995) used Galerkin method to solve the equations obtained by Hamilton's principle for nonlinear free vibration of conical sandwich shells. Shu (1996) by using love theory and GDQ studied the vibration of isotropic conical shells. Tornabene *et al*. (2009) surveyed the dynamic behavior of FG conical shells and annular plates using the first-order shear deformation theory. The governing equations of motion are discretized by means of the generalized differential quadrature (GDQ) method. Sofiyev (2012) investigated the vibration behavior of FG conical shells by applying the large deformation theory and analyzed the frequency with the Superposition method, Galerkin method and Harmonic balance method. Najafov *et al*. (2014) investigated the vibration behavior of FG truncated conical shell based on von-Karman-Donnell type nonlinear kinematic. Heydarpour *et al*. (2014) employed FSDT and DQM to analyze the free vibration of rotated truncated conical shells which made of carbon nanotube reinforced composite. Sofiyev and Kuruoglu (2015) investigated the vibration of FG conical shell under mixed conditions by means of Airy stress function method. Sofiyev (2016) studied the parametric vibration of FG truncated conical shells subjected to the different pressure loadings based on FSDT. Sofiyev and Osmancelebioglu (2017) by applying FSDT studied the vibration of sandwich truncated conical shells with FG coatings. Mouli *et al*. (2018) by using ANSYS APDL prepared a finite element model to investigate the free vibration of FG conical shells in a fully clamped condition. Kiani *et al*. (2018) studied the free vibration of composite conical panels which reinforced with FG carbon nanotube by applying FSDT and Donnell's theory. Sofiyev (2018) studied the vibration behavior of laminated conical shells by employing FSDT and Galerkin method. Shakouri (2019) investigated the vibration behavior of temperature dependent FG rotating conical shells by Donnell shell theory in thermal environments. Sofiyev (2019) in a review paper gathered some researches on vibration and buckling of FG shells.

As a result of review in the accessible literatures, it's found that there is no work on the vibration behavior of truncated conical sandwich shells with porous FG faces and homogeneous core with temperature dependent materials properties based on a modified high order sandwich shells theory in the uniform, linear and nonlinear temperature distributions. So, in this study, for the first time, by applying a high order theory which modified by considering the flexibility of the core in the thickness direction, vibration behavior of the truncated conical sandwich shells are investigated in the uniform, linear and nonlinear temperature distributions. Sandwiches consist of two FG faces which cover a homogeneous core. FGMs properties are temperature and location dependent which graded in according to power law rules that modified by considering

the volume fractions of two types of porosity. The homogeneous core is temperature dependent, too. Unlike the most papers, high order stresses and thermal stress resultants, in plane stresses and thermal stresses of the core and face sheets are considered at the same time. Nonlinear strains are used for both mechanical and thermal stresses to obtain the more accurate equations that causes the problem be more complicated. Boundary condition is simply supported and equations are derived based on the Hamilton's energy principle. To obtain the frequencies, a Galerkin method is applied. In order to validate the present approach, the results of this analytical approach are compared with the numerical results which obtained by Abaqus software and for a special case are compared with some literatures. Finally, the effects of the temperature changing, volume fraction distribution of FG face sheets, porosity and some geometrical effects on the free vibration characteristics of defined sandwich shells are investigated.

2. Theoretical formulation

2.1 Material modelling

This study investigates the vibration behavior of a truncated conical sandwich shell which functionally graded materials are applied in the face sheets. Usually FGMs are composed of metal and ceramic which in the manufacturing process some micro voids appear in these materials. The material properties of the porous FG face sheets, $P(z_j,T)$, vary gradually in the thickness direction. So, they can be modelled in accordant to the power-law rule modified with two kinds of porosity distributions between ceramic and metal. The first one is even that modifies the power law rule as follows (Boutahar and Benamar 2016)

$$P_j\left(z_j,T\right)=g\left(z_j\right)P_{ce}^{j}\left(T\right)+\left[1-g\left(z_j\right)\right]P_m^{j}\left(T\right) -(P_{ce}^{j}\left(T\right)+P_m^{j}\left(T\right))\frac{\zeta}{2}\ \square\ \square j=(o,i) \tag{1}$$

$$g\left(z_o\right)=(\frac{\frac{h_o}{2}-z_o}{h_o})^N \tag{2}$$

$$g\left(z_i\right)=(\frac{\frac{h_i}{2}+z_i}{h_i})^N \tag{3}$$

where "ζ" is the porosity volume fraction; "N" is the constant power law index; and subscripts "o" and "i" refer to outer and inner faces, respectively. It is assumed that the porosities occurred at the middle area when the FGM structures have been produced based on the principle of multi-step sequential infiltration techniques. In this area, infiltration of the material is hard and imperfect but at the edges of the FG layer it has been performed easily that causes to less porosity. So, in the second approximation, it is considered that the porosities are distributed in the middle area of the FG layer and by approaching to the edges, they decrease and tend to the zero. Therefore, the equation of the material properties in the uneven case modified as follows (Boutahar and Benamar 2016)

$$P_j\left(z_j,T\right)=g\left(z_j\right)P_{ce}^{j}\left(T\right)+\left[1-g\left(z_j\right)\right]P_m^{j}\left(T\right) -(P_{ce}^{j}\left(T\right)+P_m^{j}\left(T\right))\frac{\zeta}{2}(1-\frac{2\left|z\right|}{h}) \tag{4}$$

As seen in Eqs. (1) and (4), the face sheets material properties vary by both location and temperature. To increase the accuracy of the model, the material properties of the homogenous core must be temperature dependent, too. These properties change by a nonlinear function of the temperature as follows (Shen 2009)

$$P=P_0\left(P_{-1}T^{-1}+1+P_1T+P_2T^{2}+P_3T^{3}\right) \tag{5}$$

where $(T=T_0+\Delta T)$ and $T_0=300K$. P_0, P_{-1}, P_1, P_2 and P_3 are coefficients and unique for the constituent materials.

2.2 Temperature distribution

Three types of temperature variations, namely, uniform, linear and nonlinear are considered in this study. In order to model the linear distribution of temperature, the temperature distributions are assumed linearly through the thickness of each layer accordant to Eqs. (6)-(8).

$$T_o(z_o)=r_1z_o+r_2 \tag{6}$$

$$T_c(z_c)=r_3z_c+r_4 \tag{7}$$

$$T_i(z_i)=r_5z_i+r_6 \tag{8}$$

where r_1, r_2, r_3, r_4, r_5 and r_6 are the unknown coefficients of the polynomials that obtained with six thermal boundary conditions in Eqs. (9) and (10).

$$\begin{gathered}T_o(-h_o/2)=T_o;\quad T_o(h_o/2)=T_c(-h_c/2)\\ k_o(h_o/2,T_{io})\partial T_o/\partial z_o=k_c(-h_c/2,T_{io})\partial T_c/\partial z_c\end{gathered} \tag{9}$$

$$\begin{gathered}T_i(h_i/2)=T_i;\quad T_c(h_c/2)=T_i(-h_i/2)\\ k_i(-h_i/2,T_{ii})\partial T_i/\partial z_i=k_c(h_c/2,T_{ii})\partial T_c/\partial z_c\end{gathered} \tag{10}$$

where "k" is the thermal conductivity; "T_o" and "T_i" are the temperatures of outer and inner surfaces of the sandwiches; "T_{io}" and "T_{ii}" are the temperatures of the top and bottom interfaces of the core with outer and inner face sheets.

To model the nonlinear temperature distribution, the steady state, one dimensional heat conduction equations are considered for two face sheets and the core, separately. The nonlinear temperature rises equations of the face sheets and the core can be considered as

$$-\frac{d}{dz_o}(k_o\left(z_o\ T_o\right)\frac{dT_o}{dz_o})=0 \tag{11}$$

$$-\frac{d}{dz_c}(k_c(T_c)\frac{dT_c}{dz_c}=0 \tag{12}$$

$$-\frac{d}{dz_i}(k_i(z_i\ T_i)\frac{dT_i}{dz_i})=0 \tag{13}$$

The boundary conditions are as follows

$$T_c(h_c/2)=T_{ii};\quad T_c(-h_c/2)=T_{oi} \tag{14}$$

$$\begin{gathered}T_o(h_o/2)=T_{oi};\quad T_o(-h_o/2)=T_o\\ k_o(z_o)\partial T_o/\partial z_o\big|_{z_o=h_o/2}=k_c\,\partial T_c/\partial z_c\big|_{z_c=-h_c/2}\end{gathered} \tag{15}$$

$$\begin{gathered}T_i(-h_i/2)=T_{ii};\quad T_i(h_i/2)=T_i\\ k_i(z_i)\partial T_i/\partial z_i\big|_{z_i=-h_i/2}=k_c\,\partial T/\partial z_c\big|_{z_c=h_c/2}\end{gathered} \tag{16}$$

By using Eqs. (11)-(13) and boundary conditions in Eqs. (14)-(16), the nonlinear temperature distribution in the face sheets can be determined as Eq. (24) of reference (Talebitooti 2018) and the temperature rise in the core can be obtained by Eq. (17) as follows

$$T_c(z_c)=\left(\frac{T_{ii}-T_{oi}}{\int_{-h_c/2}^{h_c/2}\frac{dz_c}{k_c(T_{c1})}}\right)\int_{-h_c/2}^{z_c}\frac{dz_c}{k_c(T_{c1})}+T_{oi} \tag{17}$$

3. Kinematic equations

In Fig. 1, schematic of a truncated conical sandwich shell is depicted. The semi-vertex angle of the cone is depicted by "β". "h_o", "h_i" and "h_c" are the thicknesses of the layers. "R_1" and "R_2" show the small and large ends radii of the cone, respectively. Radius variation of the truncated conical shell is as follows

$$R(s)=R_1+s.sin\beta \tag{18}$$

The meridional, circumferential and normal directions of the sandwich shell are shown by s, θ and z, respectively.

Based on the high order sandwich shell theory, separate displacement fields should be considered for each layer. So, the first order shear deformation theory (FSDT) is employed to model the displacement fields of the porous FG face-sheets

$$u_j(s,\theta,z_j)=u_{0j}(s,\theta)+z_j\phi_s^j(s,\theta);\ (j=o,i) \tag{19}$$

$$v_j(s,\theta,z_j)=v_{0j}(s,\theta)+z_j\phi_\theta^j(s,\theta) \tag{20}$$

$$w_j(s,\theta,z_j)=w_{0j}(s,\theta) \tag{21}$$

where subscript "0" denotes values with correspondence to the middle surface of the layers and "ϕ" is the rotation of the normal to the middle surface. Cubic patterns are applied to model the kinematic relations of the core with twelve unknown coefficients for the in-plane and vertical displacement components as follows

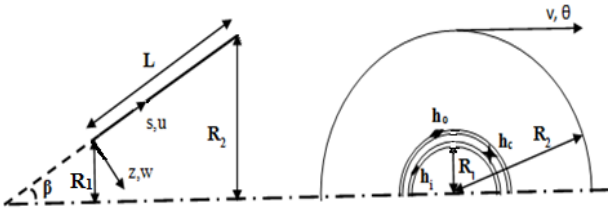

Fig. 1 Schematic of truncated conical sandwich shell

$$\begin{gathered}u_c(s,\theta,z_c,t)=u_0(s,\theta,t)+u_1(s,\theta,t)z_c+\\ u_2(s,\theta,t)z_c^2+u_3(s,\theta,t)z_c^3\end{gathered} \tag{22}$$

$$\begin{gathered}v_c(s,\theta,z_c,t)=v_0(s,\theta,t)+v_1(s,\theta,t)z_c+\\ v_2(s,\theta,t)z_c^2+v_3(s,\theta,t)z_c^3\end{gathered} \tag{23}$$

$$\begin{gathered}w_c(s,\theta,z_c,t)=w_0(s,\theta,t)+w_1(s,\theta,t)z_c+\\ w_2(s,\theta,t)z_c^2+w_3(s,\theta,t)z_c^3\end{gathered} \tag{24}$$

This study assumed that the core is sticked to the faces completely. Therefore, the compatibility conditions can be written by the interface displacements between the face sheets and the core as follows

$$\begin{gathered}u_o\left(z_o=h_o/2\right)=u_c\left(z_c=-h_c/2\right)\\ v_o\left(z_o=h_o/2\right)=v_c\left(z_c=h_c/2\right)\\ w_o=w_c\left(z_c=-h_c/2\right)\end{gathered} \tag{25}$$

$$\begin{gathered}u_c\left(z_c=h_c/2\right)=u_i\left(z_i=-h_i/2\right)\\ v_c\left(z_c=h_c/2\right)=v_i\left(z_i=-h_i/2\right)\\ w_c\left(z_c=h_c/2\right)=w_i\end{gathered} \tag{26}$$

According to von Karman nonlinear relations, the strain components of the faces sheets are defined as follows

$$\varepsilon_{ss}^j=u_{0,s}^j+z_j\phi_{s,s}^j+\frac{1}{2}(w_{0,s}^j)^2\qquad j=(o,i) \tag{27}$$

$$\begin{gathered}\varepsilon_{\theta\theta}^j=\frac{1}{r}[v_{0,\theta}^j+z_j\phi_{\theta,\theta}^j+u_0^j sin\beta+z_j\phi_s^j\sin\beta+\\ w_0^j cos\beta]+\frac{1}{2r^2}\left[w_{0,\theta}^j\right]^2\end{gathered} \tag{28}$$

$$\varepsilon_{zz}^j=0 \tag{29}$$

$$\gamma_{s\theta}^{j}=\frac{1}{r}\left[u_{0,\theta}^{j}+z_{j}\phi_{s,\theta}^{j}-v_{0}^{j}\sin\beta-z_{j}\phi_{\theta}^{j}\sin\beta\right]+ \\ v_{0,s}^{j}+z_{j}\phi_{\theta,s}^{j}+\frac{1}{r}\left[w_{0,s}^{j}w_{0,\theta}^{j}\right] \tag{30}$$

$$\gamma_{sz}^{j}=\phi_{s}^{j}+w_{0,s}^{j} \tag{31}$$

$$\gamma_{\theta z}^{j}=\frac{1}{r}\left[w_{0,\theta}^{j}-v_{0}^{j}\cos\beta-z_{j}\phi_{\theta}^{j}\cos\beta\right]+\phi_{\theta}^{j} \tag{32}$$

Similarly, the nonlinear kinematic relations of the core are determined as follows

$$\varepsilon_{ss}^{c}=u_{c,s}+\frac{1}{2}(w_{0,s})^{2} \tag{33}$$

$$\varepsilon_{\theta\theta}^{c}=\frac{1}{r}\left[v_{c,\theta}+u_{c,\theta}\sin\beta+w_{c}\cos\beta\right]+\frac{1}{2r^{2}}\left[w_{0,\theta}\right]^{2} \tag{34}$$

$$\varepsilon_{zz}^{c}=w_{c,z} \tag{35}$$

$$\gamma_{s\theta}^{c}=\frac{1}{r}\left[u_{c,\theta}-v_{c}\sin\beta\right]+v_{c,s}+\frac{1}{r}\left[w_{0,s}w_{0,\theta}\right] \tag{36}$$

$$\gamma_{sz}^{c}=u_{c,z}+w_{c,s} \tag{37}$$

$$\gamma_{\theta z}^{c}=\frac{1}{r}\left[w_{c,\theta}-v_{c}\cos\beta\right]+v_{c,z} \tag{38}$$

4. Governing equations

In order to study the vibration behavior of functionally graded conical sandwich shells and obtain the governing equations of motion, Hamilton's energy principle is applied which consists of variation of the kinetic and strain energies as follows (Reddy 2003)

$$\int_{t1}^{t2}\left(\delta K+\delta U\right)dt=0 \tag{39}$$

The variation of kinetic and strain energies are δK and δU, respectively. The variation of the kinetic energy is calculated as follows

$$\int_{t1}^{t2}\delta K dt= \\ -\int_{t1}^{t2}\{\int_{0}^{L}\int_{0}^{2\pi}\int_{-\frac{h_o}{2}}^{\frac{h_o}{2}}\rho_{o}\left(z_{o},T_{o}\right)(\ddot{u}_{o}\delta u_{o}+\ddot{\upsilon}_{o}\delta\upsilon_{o}+\ddot{w}_{o}\delta w_{o}\ rdsd\theta dz_{o} \\ +\int_{0}^{L}\int_{0}^{2\pi}\int_{-\frac{h_i}{2}}^{\frac{h_i}{2}}\rho_{i}\left(z_{i},T_{i}\right)(\ddot{u}_{i}\delta u_{i}+\ddot{\upsilon}_{i}\delta\upsilon_{i}+\ddot{w}_{i}\delta w_{i}\ rdsd\theta dz_{i} \\ +\int_{0}^{L}\int_{0}^{2\pi}\int_{-\frac{h_c}{2}}^{\frac{h_c}{2}}\rho_{c}\left(T_{c}\right)(\ddot{u}_{c}\delta u_{c}+\ddot{\upsilon}_{c}\delta\upsilon_{c}+\ddot{w}_{c}\delta w_{c}\ rdsd\theta dz_{c}\}dt \tag{40}$$

where $(\ddot{\ })$ indicates the second derivative with respect to time. The core is indicated with the subscript "c". "T" is the temperature variations. The density is "ρ" which in the face sheets is a function of displacement and temperature and in the core is just a function of temperature. The variation of the total strain energy includes all mechanical and thermal stresses and linear and nonlinear strains of the layers of sandwich shell that make the mechanical and thermal energies. In addition, the compatibility conditions at the interfaces of the core and the face-sheets attended in the Hamilton's principle as the constraints by use of six Lagrange multipliers. Finally, by considering the in-plane stresses of the core in this study, δU is as follows

$$\delta U=\int_{V_o}((\sigma_{ss}^{o}+\sigma_{ss}^{oT})\delta\varepsilon_{ss}^{o}+(\sigma_{\theta\theta}^{o}+\sigma_{\theta\theta}^{oT})\delta\varepsilon_{\theta\theta}^{o}+\tau_{s\theta}^{o}\delta\gamma_{s\theta}^{o} \\ +\tau_{sz}^{o}\delta\gamma_{sz}^{o}+\tau_{\theta z}^{o}\delta\gamma_{\theta z}^{o})dV_{o}+\int_{V_i}((\sigma_{ss}^{i}+\sigma_{ss}^{iT})\delta\varepsilon_{ss}^{i}+ \\ (\sigma_{\theta\theta}^{i}+\sigma_{\theta\theta}^{iT})\delta\varepsilon_{\theta\theta}^{i}+\tau_{s\theta}^{i}\delta\gamma_{s\theta}^{i}+\tau_{sz}^{i}\delta\gamma_{sz}^{i}+\tau_{\theta z}^{i}\delta\gamma_{\theta z}^{i})dV_{i} \\ +\int_{V_c}((\sigma_{ss}^{c}+\sigma_{ss}^{cT})\delta\varepsilon_{ss}^{c}+(\sigma_{\theta\theta}^{c}+\sigma_{\theta\theta}^{cT})\delta\varepsilon_{\theta\theta}^{c}+(\sigma_{zz}^{c}+\sigma_{zz}^{cT})\delta\varepsilon_{zz}^{c}+ \\ \tau_{s\theta}^{c}\delta\gamma_{s\theta}^{c}+\tau_{sz}^{c}\delta\gamma_{sz}^{c}+\tau_{\theta z}^{c}\delta\gamma_{\theta z}^{c})dV_{c}+ \\ \delta\int_{0}^{L}\int_{0}^{2\pi}[\lambda_{so}\left(u_{o}\left(z_{o}=h_{o}/2\right)-u_{c}\left(z_{c}=-h_{c}/2\right)\right) \\ +\lambda_{\theta o}\left(\upsilon_{o}\left(z_{o}=h_{o}/2\right)-\upsilon_{c}\left(z_{c}=-h_{c}/2\right)\right)+ \\ \lambda_{zo}\left(w_{o}\left(z_{o}=h_{o}/2\right)-w_{c}\left(z_{c}=-h_{c}/2\right)\right)+ \\ \lambda_{si}\left(u_{c}\left(z_{c}=h_{c}/2\right)-u_{i}\left(z_{i}=-h_{i}/2\right)\right)+ \\ \lambda_{\theta i}\left(\upsilon_{c}\left(z_{c}=h_{c}/2\right)-\upsilon_{i}\left(z_{i}=-h_{i}/2\right)\right)+ \\ \lambda_{zi}\left(w_{c}\left(z_{c}=h_{c}/2\right)-w_{i}\right)]rdsd\theta \tag{41}$$

where σ_{ss}, $\sigma_{\theta\theta}$ and $\tau_{s\theta}$ display the in-plane normal and shear stresses; ε_{ss}, $\varepsilon_{\theta\theta}$ and $\gamma_{s\theta}$ are the in plane normal and shear strains of the layers; σ_{ss}^{T} and $\sigma_{\theta\theta}^{T}$ express the thermal stresses; σ_{zz}^{c} and ε_{zz}^{c} present the lateral normal stress and strain in the core; τ_{sz}^{c}, $\tau_{\theta z}^{c}$, γ_{sz}^{c} and $\gamma_{\theta z}^{c}$ declare shear stresses and shear strains in the core; and λ_{s}, λ_{θ} and λ_{z} are the Lagrange multipliers at the face sheet-core interfaces. For expanding Eqs. (40)-(41), some basic relations and expresses must be introduced to determine the stress and moment resultants for the face sheets as

$$\begin{bmatrix} N_{ss}^{j} \\ N_{\theta\theta}^{j} \\ N_{s\theta}^{j} \\ M_{ss}^{j} \\ M_{\theta\theta}^{j} \\ M_{s\theta}^{j} \end{bmatrix} = \begin{bmatrix} A_{11}^{j} & A_{12}^{j} & 0 & B_{11}^{j} & B_{12}^{j} & 0 \\ A_{12}^{j} & A_{22}^{j} & 0 & B_{12}^{j} & B_{22}^{j} & 0 \\ 0 & 0 & A_{66}^{j} & 0 & 0 & B_{66}^{j} \\ B_{11}^{j} & B_{12}^{j} & 0 & D_{11}^{j} & D_{12}^{j} & 0 \\ B_{12}^{j} & B_{22}^{j} & 0 & D_{12}^{j} & D_{22}^{j} & 0 \\ 0 & 0 & B_{66}^{j} & 0 & 0 & D_{66}^{j} \end{bmatrix} \begin{bmatrix} \varepsilon_{ss}^{0} \\ \varepsilon_{\theta\theta}^{0} \\ \varepsilon_{s\theta}^{0} \\ k_{ss} \\ k_{\theta\theta} \\ k_{s\theta} \end{bmatrix} - \begin{bmatrix} N_{ss}^{Tj} \\ N_{\theta\theta}^{Tj} \\ 0 \\ M_{ss}^{Tj} \\ M_{\theta\theta}^{Tj} \\ 0 \end{bmatrix} \quad (42)$$

$$, j = (o, i)$$

$$\begin{bmatrix} Q_{sj}^{0} \\ Q_{\theta j}^{0} \end{bmatrix} = \frac{\pi^2}{12} \begin{bmatrix} A_{44}^{j} & 0 \\ 0 & A_{55}^{j} \end{bmatrix} \begin{bmatrix} \gamma_{szj}^{0} \\ \gamma_{\theta zj}^{0} \end{bmatrix} + \frac{\pi^2}{12} \begin{bmatrix} B_{44}^{j} & 0 \\ 0 & B_{55}^{j} \end{bmatrix} \begin{bmatrix} \gamma_{szj}^{1} \\ \gamma_{\theta zj}^{1} \end{bmatrix} \quad (43)$$

$$Q_{\theta j}^{1} = \frac{\pi^2}{12} B_{55}^{j} \gamma_{\theta zj}^{0} + \frac{\pi^2}{12} D_{55}^{j} \gamma_{\theta zj}^{1}$$

where the "N"s and "N^T"s depict the in-plane stress resultants and thermal stress resultants, respectively; "Q"s declare the out of plane shear stress resultants; "M"s and "M^T"s refer to the moment resultants and thermal moment resultants, respectively; and, the constant coefficients A_{kl}^{j}, B_{kl}^{j} and D_{kl}^{j} indicate the stretching, bending-stretching, and bending stiffnesses, respectively, which defined in reference (Reddy 2003). Also, the high order thermal stress resultants of the face sheets and the core that appear in the equations are defined as follows

$$\begin{Bmatrix} N_{ss}^{jT} \\ M_{ss}^{jT} \end{Bmatrix} = \begin{Bmatrix} N_{\theta\theta}^{jT} \\ M_{\theta\theta}^{jT} \end{Bmatrix} = \int_{-hj/2}^{hj/2} \left(\frac{E_j(z_j, T_j)}{1 - \nu_j(z_j, T_j)} \alpha_j(z_j, T_j) T_j \right) \begin{Bmatrix} 1 \\ z_j \end{Bmatrix} dz_j$$

$$\begin{Bmatrix} R_{ss}^{cT} \\ M_{s1}^{cT} \\ M_{s2}^{cT} \\ M_{s3}^{cT} \end{Bmatrix} = \begin{Bmatrix} R_{\theta\theta}^{cT} \\ M_{t1}^{cT} \\ M_{t2}^{cT} \\ M_{t3}^{cT} \end{Bmatrix} = \begin{Bmatrix} R_{zz}^{cT} \\ M_{z1}^{cT} \\ M_{z2}^{cT} \end{Bmatrix} = \int_{-hc/2}^{hc/2} \left(\frac{E_c(T_c)}{1 - \nu_c(T_c)} \alpha_c(T_c) T_c \right) \begin{Bmatrix} 1 \\ z_c \\ z_c^{\,2} \\ z_c^{\,3} \end{Bmatrix} dz_c \quad (44)$$

$$j = (o, i)$$

Where E, v and α are the Young's modulus, the Poisson's ratio and the thermal expansion coefficient, respectively. By substituting the kinematic relations and compatibility conditions, and after some algebraic operations, the twenty eight equations of motion are obtained. These equations include twenty eight unknowns: ten displacement unknowns for face sheets, twelve displacement unknowns for the core, and six Lagrange multipliers as follows

$$-I_{0o} r \ddot{u}_0^o - I_{1o} r \ddot{\phi}_s^o - N_{ss}^o \sin\beta - r N_{ss,s}^o - N_{ss}^{oT} \sin\beta - r N_{ss,s}^{oT} + N_{\theta\theta}^o \sin\beta + N_{\theta\theta}^{oT} \sin\beta - N_{s\theta,\theta}^o + r\lambda_{so} = 0 \quad (45)$$

$$-I_{0o} r \ddot{v}_0^o - I_{1o} r \ddot{\phi}_\theta^o - N_{\theta\theta,\theta}^o - N_{\theta\theta,\theta}^{oT} - 2N_{s\theta}^o \sin\beta - r N_{s\theta,s}^o - Q_{\theta 0}^o \cos\beta + r\lambda_{\theta o} = 0 \quad (46)$$

$$-I_{0o} r \ddot{w}_0^o - N_{ss}^o \sin\beta w_{0,s}^o - N_{ss,s}^o r w_{0,s}^o - N_{ss}^o r w_{0,ss}^o - N_{ss}^{oT} \sin\beta w_{0,s}^o - N_{ss,s}^{oT} r w_{0,s}^o - N_{ss}^{oT} r w_{0,ss}^o + N_{\theta\theta}^o \cos\beta - r^{-1} N_{\theta\theta,\theta}^o w_{0,\theta}^o - r^{-1} N_{\theta\theta}^o w_{0,\theta\theta}^o + N_{\theta\theta}^{oT} \cos\beta - r^{-1} N_{\theta\theta,\theta}^{oT} w_{0,\theta}^o - r^{-1} N_{\theta\theta}^{oT} w_{0,\theta\theta}^o - N_{s\theta,s}^o w_{0,\theta}^o - 2N_{s\theta}^o w_{0,s\theta}^o - N_{s\theta,\theta}^o w_{0,s}^o - Q_{s0}^o \sin\beta - r Q_{s0,s}^o - Q_{\theta 0,\theta}^o + r\lambda_{zo} = 0 \quad (47)$$

$$-I_{1o} r \ddot{u}_0^o - I_{2o} r \ddot{\phi}_s^o - M_{ss}^o \sin\beta - r M_{ss,s}^o - M_{ss}^{oT} \sin\beta - r M_{ss,s}^{oT} + M_{\theta\theta}^o \sin\beta + M_{\theta\theta}^{oT} \sin\beta - M_{s\theta,\theta}^o + r Q_{s0}^o + r \frac{h_o}{2} \lambda_{so} = 0 \quad (48)$$

$$-I_{1o} r \ddot{v}_0^o - I_{2o} r \ddot{\phi}_\theta^o - M_{\theta\theta,\theta}^o - M_{\theta\theta,\theta}^{oT} - 2M_{s\theta}^o \sin\beta - r M_{s\theta,s}^o - Q_{\theta 1}^o \cos\beta + r Q_{\theta 0}^o + r \frac{h_o}{2} \lambda_{\theta o} = 0 \quad (49)$$

$$-I_{0i} r \ddot{u}_0^i - I_{1i} r \ddot{\phi}_s^i - N_{ss}^i \sin\beta - r N_{ss,s}^i - N_{ss}^{iT} \sin\beta - r N_{ss,s}^{iT} + N_{\theta\theta}^i \sin\beta + N_{\theta\theta}^{iT} \sin\beta - N_{s\theta,\theta}^i - r\lambda_{si} = 0 \quad (50)$$

$$-I_{0i} r \ddot{v}_0^i - I_{1i} r \ddot{\phi}_\theta^i - N_{\theta\theta,\theta}^i - N_{\theta\theta,\theta}^{iT} - 2N_{s\theta}^i \sin\beta - r N_{s\theta,s}^i - Q_{\theta 0}^i \cos\beta - r\lambda_{\theta i} = 0 \quad (51)$$

$$-I_{0i} r \ddot{w}_0^i - N_{ss}^i \sin\beta w_{0,s}^i - N_{ss,s}^i r w_{0,s}^i - N_{ss}^i r w_{0,ss}^i - N_{ss}^{iT} \sin\beta w_{0,s}^i - N_{ss,s}^{iT} r w_{0,s}^i - N_{ss}^{iT} r w_{0,ss}^i + N_{\theta\theta}^i \cos\beta - r^{-1} N_{\theta\theta,\theta}^i w_{0,\theta}^i - r^{-1} N_{\theta\theta}^i w_{0,\theta\theta}^i + N_{\theta\theta}^{iT} \cos\beta - r^{-1} N_{\theta\theta,\theta}^{iT} w_{0,\theta}^i - r^{-1} N_{\theta\theta}^{iT} w_{0,\theta\theta}^o - N_{s\theta,s}^i w_{0,\theta}^i - 2N_{s\theta}^i w_{0,s\theta}^i - N_{s\theta,\theta}^i w_{0,s}^i - Q_{s0}^i \sin\beta - r Q_{s0,s}^i - Q_{\theta 0,\theta}^i - r\lambda_{zi} = 0 \quad (52)$$

$$-I_{1i} r \ddot{u}_0^i - I_{2i} r \ddot{\phi}_s^i - M_{ss}^i \sin\beta - r M_{ss,s}^i - M_{ss}^{iT} \sin\beta - r M_{ss,s}^{iT} + M_{\theta\theta}^i \sin\beta + M_{\theta\theta}^{iT} \sin\beta - M_{s\theta,\theta}^i + r Q_{s0}^i + r \frac{h_i}{2} \lambda_{si} = 0 \quad (53)$$

$$-I_{1i} r \ddot{v}_0^i - I_{2i} r \ddot{\phi}_\theta^i - M_{\theta\theta,\theta}^i - M_{\theta\theta,\theta}^{iT} - 2M_{s\theta}^i \sin\beta - r M_{s\theta,s}^i - Q_{\theta 1}^i \cos\beta + r Q_{\theta 0}^i + r \frac{h_i}{2} \lambda_{\theta i} = 0 \quad (54)$$

$$-I_{0c} r \ddot{u}_0^c - I_{1c} r \ddot{u}_1^c - I_{2c} r \ddot{u}_2^c - I_{3c} r \ddot{u}_3^c - R_s^c \sin\beta - r R_{s,s}^c - R_s^{cT} \sin\beta - r R_{s,s}^{cT} + R_\theta^c \sin\beta + R_\theta^{cT} \sin\beta - Q_{s\theta,\theta}^c - r\lambda_{so} + r\lambda_{si} = 0 \quad (55)$$

$$-I_{1c}r\ddot{u}_0^c - I_{2c}r\ddot{u}_1^c - I_{3c}r\ddot{u}_2^c - I_{4c}r\ddot{u}_3^c - M_{s1}^c \sin\beta - rM_{s1,s}^c - M_{s1}^{cT}\sin\beta - rM_{s1,s}^{cT} + M_{\theta 1}^c \sin\beta + M_{\theta 1}^{cT}\sin\beta + rQ_{sz}^c - M_{Q1s\theta,\theta}^c + r\frac{h_c}{2}\lambda_{so} + r\frac{h_c}{2}\lambda_{si} = 0 \quad (56)$$

$$-I_{2c}r\ddot{u}_0^c - I_{3c}r\ddot{u}_1^c - I_{4c}r\ddot{u}_2^c - I_{5c}r\ddot{u}_3^c - M_{s2}^c \sin\beta - rM_{s2,s}^c - M_{s2}^{cT}\sin\beta - rM_{s2,s}^{cT} + M_{\theta 2}^c \sin\beta + M_{\theta 2}^{cT}\sin\beta + 2rM_{Q1sz}^c - M_{Q2s\theta,\theta}^c - r\frac{h_c^2}{4}\lambda_{so} + r\frac{h_c^2}{4}\lambda_{si} = 0 \quad (57)$$

$$-I_{3c}r\ddot{u}_0^c - I_{4c}r\ddot{u}_1^c - I_{5c}r\ddot{u}_2^c - I_{6c}r\ddot{u}_3^c - M_{s3}^c \sin\beta - rM_{s3,s}^c - M_{s3}^{cT}\sin\beta - rM_{s3,s}^{cT} + M_{\theta 3}^c \sin\beta + M_{\theta 3}^{cT}\sin\beta + 3rM_{Q2sz}^c - M_{Q3s\theta,\theta}^c + r\frac{h_c^3}{8}\lambda_{so} + r\frac{h_c^3}{8}\lambda_{si} = 0 \quad (58)$$

$$-I_{0c}r\ddot{v}_0^c - I_{1c}r\ddot{v}_1^c - I_{2c}r\ddot{v}_2^c - I_{3c}r\ddot{v}_3^c - R_{\theta,\theta}^c - R_{\theta,\theta}^{cT} - Q_{\theta z}^c \cos\beta - 2Q_{s\theta}^c \sin\beta - rQ_{s\theta,s}^c - r\lambda_{\theta o} + r\lambda_{\theta i} = 0 \quad (59)$$

$$-I_{1c}r\ddot{v}_0^c - I_{2c}r\ddot{v}_1^c - I_{3c}r\ddot{v}_2^c - I_{4c}r\ddot{v}_3^c - M_{\theta 1,\theta}^c - M_{\theta 1,\theta}^{cT} - M_{Q1\theta z}^c \cos\beta + rQ_{\theta z}^c - 2M_{Q1s\theta}^c \sin\beta - rM_{Q1s\theta,s}^c + r\frac{h_c}{2}\lambda_{\theta o} + r\frac{h_c}{2}\lambda_{\theta i} = 0 \quad (60)$$

$$-I_{2c}r\ddot{v}_0^c - I_{3c}r\ddot{v}_1^c - I_{4c}r\ddot{v}_2^c - I_{5c}r\ddot{v}_3^c - M_{\theta 2,\theta}^c - M_{\theta 2,\theta}^{cT} - M_{Q2\theta z}^c \cos\beta + 2rM_{Q1\theta z}^c - 2M_{Q2s\theta}^c \sin\beta - rM_{Q2s\theta,s}^c + r\frac{h_c^2}{4}\lambda_{\theta o} + r\frac{h_c^2}{4}\lambda_{\theta i} = 0 \quad (61)$$

$$-I_{3c}r\ddot{v}_0^c - I_{4c}r\ddot{v}_1^c - I_{5c}r\ddot{v}_2^c - I_{6c}r\ddot{v}_3^c - M_{\theta 3,\theta}^c - M_{\theta 3,\theta}^{cT} - M_{Q3\theta z}^c \cos\beta + 3rM_{Q2\theta z}^c - 2M_{Q3s\theta}^c \sin\beta - rM_{Q3s\theta,s}^c + r\frac{h_c^3}{8}\lambda_{\theta o} + r\frac{h_c^3}{8}\lambda_{\theta i} = 0 \quad (62)$$

$$-I_{0c}r\ddot{w}_0^c - I_{1c}r\ddot{w}_1^c - I_{2c}r\ddot{w}_2^c - I_{3c}r\ddot{w}_3^c - R_s^c \sin\beta w_{0,s}^c - R_{s,s}^c r w_{0,s}^c - R_s^c r w_{0,ss}^c - R_s^{cT}\sin\beta w_{0,s}^c - R_{s,s}^{cT} r w_{0,s}^c - R_s^{cT} r w_{0,ss}^c + R_\theta^c \cos\beta - r^{-1}R_{\theta,\theta}^c w_{0,\theta}^c - r^{-1}R_\theta^c w_{0,\theta\theta}^c + R_\theta^{cT}\cos\beta - r^{-1}R_{\theta,\theta}^{cT} w_{0,\theta}^c - r^{-1}R_\theta^{cT} w_{0,\theta\theta}^c - Q_{sz}^c \sin\beta - rQ_{sz,s}^c - Q_{\theta z,\theta}^c - Q_{s\theta,s}^c w_{0,\theta}^c - -2Q_{s\theta}^c w_{0,s\theta}^c - Q_{s\theta,\theta}^c w_{0,s}^c - r\lambda_{zo} + r\lambda_{zi} = 0 \quad (63)$$

$$-I_{1c}r\ddot{w}_0^c - I_{2c}r\ddot{w}_1^c - I_{3c}r\ddot{w}_2^c - I_{4c}r\ddot{w}_3^c + M_{\theta 1}^c \cos\beta + M_{\theta 1}^{cT}\cos\beta + rR_z^c + rR_z^{cT} - M_{Q1sz}^c \sin\beta - rM_{Q1sz,s}^c - M_{Q1\theta z,\theta}^c + r\frac{h_c}{2}\lambda_{zo} + r\frac{h_c}{2}\lambda_{zi} = 0 \quad (64)$$

$$-I_{2c}r\ddot{w}_0^c - I_{3c}r\ddot{w}_1^c - I_{4c}r\ddot{w}_2^c - I_{5c}r\ddot{w}_3^c + M_{\theta 2}^c \cos\beta + M_{\theta 2}^{cT}\cos\beta + 2rM_{z1}^c + 2rM_{z1}^{cT} - M_{Q2sz}^c \sin\beta - rM_{Q2sz,s}^c - M_{Q2\theta z,\theta}^c - r\frac{h_c^2}{4}\lambda_{zo} + r\frac{h_c^2}{4}\lambda_{zi} = 0 \quad (65)$$

$$-I_{3c}r\ddot{w}_0^c - I_{4c}r\ddot{w}_1^c - I_{5c}r\ddot{w}_2^c - I_{6c}r\ddot{w}_3^c + M_{\theta 3}^c \cos\beta + M_{\theta 3}^{cT}\cos\beta + 3rM_{z2}^c + 3rM_{z2}^{cT} - M_{Q3sz}^c \sin\beta - rM_{Q3sz,s}^c - M_{Q3\theta z,\theta}^c + r\frac{h_c^3}{8}\lambda_{zo} + r\frac{h_c^3}{8}\lambda_{zi} = 0 \quad (66)$$

$$u_{0o} + \frac{h_o}{2}\phi_s^o - u_{0c} + \frac{h_c}{2}u_{1c} - \frac{h_c^2}{4}u_{2c} + \frac{h_c^3}{8}u_{3c} = 0 \quad (67)$$

$$v_{0o} + \frac{h_o}{2}\phi_\theta^o - v_{0c} + \frac{h_c}{2}v_{1c} - \frac{h_c^2}{4}v_{2c} + \frac{h_c^3}{8}v_{3c} = 0 \quad (68)$$

$$w_{0o} - w_{0c} + \frac{h_c}{2}w_{1c} - \frac{h_c^2}{4}w_{2c} + \frac{h_c^3}{8}w_{3c} = 0 \quad (69)$$

$$u_{0c} + \frac{h_c}{2}u_{1c} + \frac{h_c^2}{4}u_{2c} + \frac{h_c^3}{8}u_{3c} - u_{0i} + \frac{h_i}{2}\phi_s^i = 0 \quad (70)$$

$$v_{0c} + \frac{h_c}{2}v_{1c} + \frac{h_c^2}{4}v_{2c} + \frac{h_c^3}{8}v_{3c} - v_{0i} + \frac{h_o}{2}\phi_\theta^i = 0 \quad (71)$$

$$w_{0c} + \frac{h_c}{2}w_{1c} + \frac{h_c^2}{4}w_{2c} + \frac{h_c^3}{8}w_{3c} - w_{0i} = 0 \quad (72)$$

where, the inertia terms of the FG face sheets and the core are calculated as follows

$$\left(I_{0j}, I_{1j}, I_{2j}\right) = \int_{-hj/2}^{hj/2} \rho_j \left(z_j, T_j\right)\left(1, z_j, z_j^2\right)dz_j, ? \quad (j = o\ \ i) \quad (73)$$

$$\left(I_{0c}, I_{1c}, I_{2c}, I_{3c}, I_{4c}, I_{5c}, I_{6c}\right) = \int_{-hc/2}^{hc/2} \rho_c \left(T_c\right)\left(1, z_c, z_c^2, z_c^3, z_c^4, z_c^5, z_c^6\right)dz_c \quad (74)$$

Also, the out-of-plane and in plane stresses of the core leads to the high order resultants which are calculated as

$$Q_{sc}, M_{Q1sz}, M_{Q2sz}, M_{Q3sz} = \int_{-hc/2}^{hc/2} \left(1, z_c, z_c^2, z_c^3\right)\tau_{sz}^c dz_c \quad (75)$$

$$Q_{\theta z}, M_{Q1\theta z}, M_{Q2\theta z}, M_{Q3\theta z} = \int_{-hc/2}^{hc/2} \left(1, z_c, z_c^2, z_c^3\right)\tau_{\theta z}^c dz_c \quad (76)$$

$$R_z, M_{z1}, M_{z2} = \int_{-hc/2}^{hc/2} (1, z_c)\sigma_{zz}^c dz_c \quad (77)$$

$$Q_{s\theta}^c, M_{Q1s\theta}^c, M_{Q2s\theta}^c, M_{Q3s\theta}^c = \int_{-hc/2}^{hc/2} (1, z_c, z_c^2, z_c^3)\tau_{s\theta}^c dz_c \quad (78)$$

$$R_s^c, M_{s1}^c, M_{s2}^c, M_{s3}^c = \int_{-hc/2}^{hc/2} (1, z_c, z_c^2, z_c^3)\sigma_{ss}^c dz_c \quad (79)$$

$$Q_{s\theta}^c, M_{Q1s\theta}^c, M_{Q2s\theta}^c, M_{Q3s\theta}^c = \int_{-hc/2}^{hc/2} (1, z_c, z_c^2, z_c^3)\tau_{s\theta}^c dz_c \quad (80)$$

Finally, by substituting the high order stress resultants in equations of motion in terms of the displacement components, the governing equations are derived in terms of the twenty eight unknowns. In the following, vibration problem of truncated conical sandwich shells with a simply support boundary conditions are solved by a Galerkin method in this study.

5. Simply supported truncated conical sandwich shell

In order to solve the governing equations of the free vibration of simply supported truncated conical sandwich shell, a Galerkin method with twenty eight trigonometric shape functions, which satisfy the boundary conditions is determined. The shape functions can be expressed as

$$u_{0k} = C_{uk} cos(a_m s)\cos(n\theta)e^{i\omega t}, k = (o, i, c) \quad (81)$$

$$v_{0k} = C_{vk} sin(a_m s)\sin(n\theta)e^{i\omega t} \quad (82)$$

$$w_{0k} = C_{wk} sin(a_m s)\cos(n\theta)e^{i\omega t} \quad (83)$$

$$\phi_s^j = C_{\phi sj} cos(a_m s)\cos(n\theta)e^{i\omega t}, j = (o, i) \quad (84)$$

$$\phi_\theta^j = C_{\phi\theta j} sin(a_m s)\sin(n\theta)e^{i\omega t} \quad (85)$$

$$\lambda_{sj} = C_{\lambda sj} cos(a_m s)\cos(n\theta)e^{i\omega t} \quad (86)$$

$$\lambda_{\theta j} = C_{\lambda\theta j} sin(a_m s)\sin(n\theta)e^{i\omega t} \quad (87)$$

$$\lambda_{zj} = C_{\lambda zj} sin(a_m s)\cos(n\theta)e^{i\omega t} \quad (88)$$

where $a_m = m\pi/L$; m and n are the wave numbers and $C_{uk}, C_{vk}, C_{wk}, C_{\phi sj}, C_{\phi\theta j}\ C_{\lambda sj}, C_{\lambda\theta j}$ and $C_{\lambda zj}$ are the twenty eight unknown constants of the shape functions. These twenty eight equations are not independent and the number of them can be reduced by a reduction approach. Lagrange constants can be isolated as the expression of the face sheets. It's seen that based on the compatibility conditions, the unknown constants of the faces are dependent to the core constants. At last by some operations, the number of the equations are reduced to sixteen in terms of the core unknown constants. These sixteen equations can be written in a 16×16 matrix which include the mass, *M*, and stiffness, *K*, matrices as follows

$$(k_{mn} - \omega_{mn}^2 M_{mn})C_{mn} = 0 \quad (89)$$

In Eq. (89), ω_{mn} is the natural frequency; and C_{mn} is the Eigen vector which contains sixteen unknown constants of the core.

6. Verification and numerical results

In order to validate the approach of this study, present results are compared with FEM results of Abaqus software and in a special case are compared with results of literature (Li *et al*. 2009). Consider an isotropic conical shell which made of aluminum with structural parameters such as h = 0.004 m, h/R_2 = 0.01, $(L)sin(\beta)/R_2$ = 0.25. These comparisons are shown in Table 1 for three values of β.

Because, theory and solution method of the present analysis are different with reference (Li *et al*. 2009), a discrepancy is found in the results.

Furthermore, in order to more investigation of the present approach, other numerical problems have been studied. Consider a simply supported FG truncated sandwich shell which interior surface of the faces as well as the core layer are made of the zirconium dioxide and the outer surface of the faces are made of silicon nitride. The properties of these materials are available in reference (Reddy 1998). Variation of the material properties in each face sheet is correspond to the modified power-law function. Numerical examples are simulated by Abaqus software for validation of the present approach as shown in Fig. 2.

In this study, results are shown by a non-dimensional parameter named fundamental frequency parameter which is defined as follows

$$\bar{\omega} = \omega h\sqrt{\frac{\rho_0}{E_0}} \quad (90)$$

where $\bar{\omega}$ is the non-dimensional fundamental frequency parameter, h is the total thickness of sandwich shell which consists two FG faces as well as core; ρ_0 is density and equal to 1kg/m^3; and E_0 is the young module equal to 1 GPa.

Table 1 Fundamental frequency parameters of present (Li *et al*. 2009) and Abaqus results

	FEM result (Li *et al*. 2009)		Present method	Abaqus
	Lam and Li	Feng-Ming Li		
$\beta = 30$	0.8420	0.8431	0.886163	0.8579
$\beta = 45$	0.7655	0.7642	0.760881	0.7648
$\beta = 60$	0.6348	0.6342	0.615840	0.6295

Fig. 2 FE model simulated by ABAQUS

Table 2 Fundamental frequency parameters of present and Abaqus results for 2-1-2 and 1-8-1 sandwiches

	N	The fundamental frequency parameter		
		Present method	Abaqus	Discrepancy (%)
2-1-2	0	3.2247	3.0265	6.54
	0.2	3.0573	2.8165	8.54
	1	2.7268	2.5702	6.09
	2	2.5618	2.3813	7.58
	∞	1.9232	2.1234	9.42
1-8-1	0	2.4318	2.3042	5.53
	0.2	2.3900	2.2236	7.48
	1	2.3060	2.1482	7.34
	2	2.2636	2.0871	8.45
	∞	1.8923	1.8634	8.10

In Table 2 fundamental frequency parameters of this approach are compared with the FEM results by Abaqus software in the temperature of the room and for different power law indices in the case of 2-1-2 and 1-8-1 sandwiches. In general, h_o-h_c-h_i sandwich shell is a structure with the indices of outer face sheet thickness, core thickness and inner face sheet thickness equal to h_o, h_c and h_i, respectively. Therefore, in 2-1-2 sandwich, every face sheet thicknesses is two times of the core thickness and the structure is symmetric and in 1-8-1 sandwich, the core thickness is eight times of the every face sheet thickness.

In Table 2 the discrepancies between the present results and FEM results are due to simulation method of FG face-sheets in Abaqus software. In order to simulate the FG face-sheets in Abaqus, every face-sheets are divided to 20 layers that each layer has different properties according to power law function. There is a good agreement between the present study results and the FEM results obtained by Abaqus.

The fundamental frequency parameter varies with temperature changing in Fig. 3. Fig. 3 is plotted in a uniform temperature distribution for 2-1-2 and 1-8-1 simply supported truncated conical FG sandwich shells in different power law indices. As shown in Fig. 3, while the temperature is increased, the fundamental frequency parameter decreases. According to Eq. (5), temperature rising reduces the strength of the material. To clarify this phenomena, in Table 3 the effect of temperature on the Young's modulus of ceramic and metal is indicated. With increasing the temperature, modulus of metal and ceramic are decreased, but due to the microstructural reasons, decreasing the module of metal is more. So, increasing the temperature reduces the mechanical properties that is one of the most important reason in decreasing the frequency in high temperature. Also, Fig. 3 depicts that in a constant temperature, the fundamental frequency decreases by increasing the gradient index. Because, with increasing the power-law index the properties of the face-sheets are tending to metal and the total strength of the structure is decreased. As shown in Fig. 3, the values of the fundamental frequencies in 2-1-2 are more than 1-8-1 for all power law indices, because the ceramic quantity of the FG

Table 3 Effect of temperature variation on the Young modulus in metal and ceramics

T	Silicon nitride	Zirconium dioxide
300 K	322.27 (GPa)	168.06 (GPa)
1500 K	252.14 (Gpa)	105.68 (GPa)
Change	21.76%	37.11%

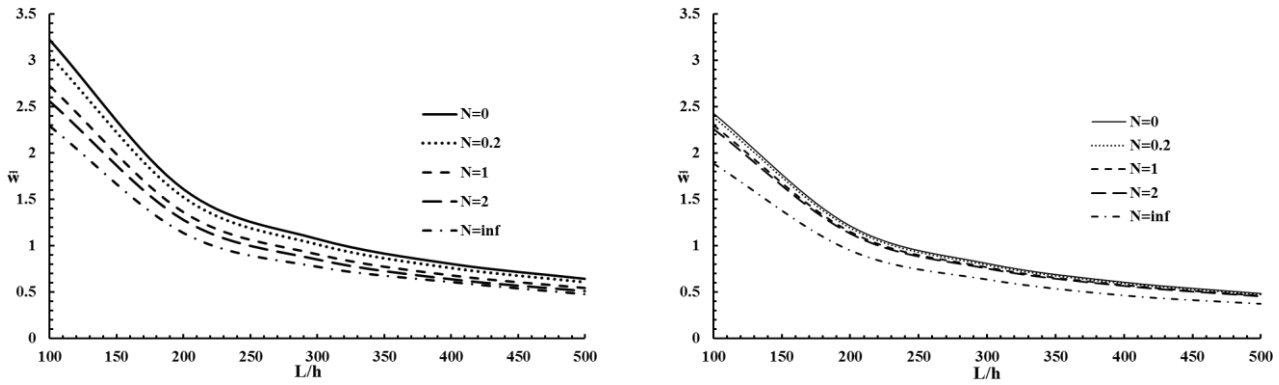

(a) 2-1-2 conical sandwich shells

(b) 1-8-1 conical sandwich shells

Fig. 3 Fundamental frequency versus temperature in various power law indices

faces in 2-1-2 is more than 1-8-1. In higher temperature 1-8-1 sandwich is too weaker than 2-1-2 one, and the fundamental frequency in 1-8-1 is tending to zero.

Now, it's time to discuss about some geometrical effects on the fundamental frequency of truncated conical sandwich shells. Fig. 4 shows the effect of length to thickness ratio on the fundamental frequency parameter for 2-1-2 and 1-8-1 truncated conical FG sandwich shells. This figure implies that when ratios are increased in a constant N, the fundamental frequency parameter decreases. Based on the Fig. 4, in the values less than 250, the slope of the fundamental frequency variation in 2-1-2 is more than 1-8-1. But, in larger ratios, this slope is almost equal. With increasing of this ratio, the stability of the structure is reduced and it is important to consider that long length is not proper for the truncated conical sandwich shells. Variation of the semi vertex angle is one of the most important geometrical effects in the cone.

In Fig. 5, the effect of the semi vertex angle on fundamental frequency parameter for 2-1-2 and 1-8-1 conical FG sandwich shells is investigated. This figure implies that with increasing the angle in a constant power law index, the fundamental frequency parameter decreases. In smaller angles, the fundamental frequency parameters of 2-1-2 sandwich are more than 1-8-1 one, but in larger angles, and especially in larger power law indices, there are little discrepancies between two types of sandwiches. As shown in Fig. 5, the results of 1-8-1 sandwich for different power law indices are close to each other, that shows the effects of the material properties variation of faces in 1-8-1 sandwich are less than 2-1-2 one.

Table 4 shows the effect of radius to thickness ratio on fundamental frequency parameter for 2-1-2 and 1-8-1 FG conical sandwich shells. The results imply that with increasing the radius to thickness ratio, the fundamental frequency parameters decrease. As depicted in Table 4, for smaller ratios with lower power law indices, the funda-

Table 4 Variation of the fundamental frequency with radius to thickness ratio for 2-1-2 and 1-8-1 sandwiches

	R_1/h	The fundamental frequency parameter				
		100	200	300	400	500
2-1-2	$N = 0$	1.6123	0.8062	0.5375	0.4031	0.3225
	$N = 0.2$	1.5286	0.7643	0.5036	0.3911	0.3003
	$N = 1$	1.3633	0.6817	0.4545	0.3409	0.2727
	$N = 2$	1.2809	0.6405	0.4270	0.3203	0.2562
1-8-1	$N = 0$	1.2159	0.6080	0.4053	0.3040	0.2432
	$N = 0.2$	1.1950	0.5976	0.3984	0.2988	0.2390
	$N = 1$	1.1530	0.5766	0.3844	0.2883	0.2306
	$N = 2$	1.1318	0.5660	0.3773	0.2830	0.2264

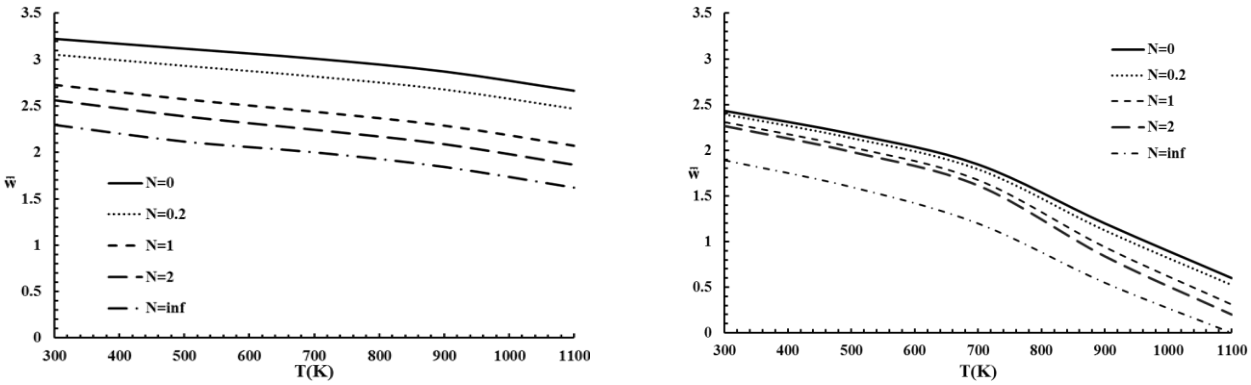

(a) 2-1-2 conical sandwich shells (b) 1-8-1 conical sandwich shells

Fig. 4 Variation of the fundamental frequency with length to thickness ratio

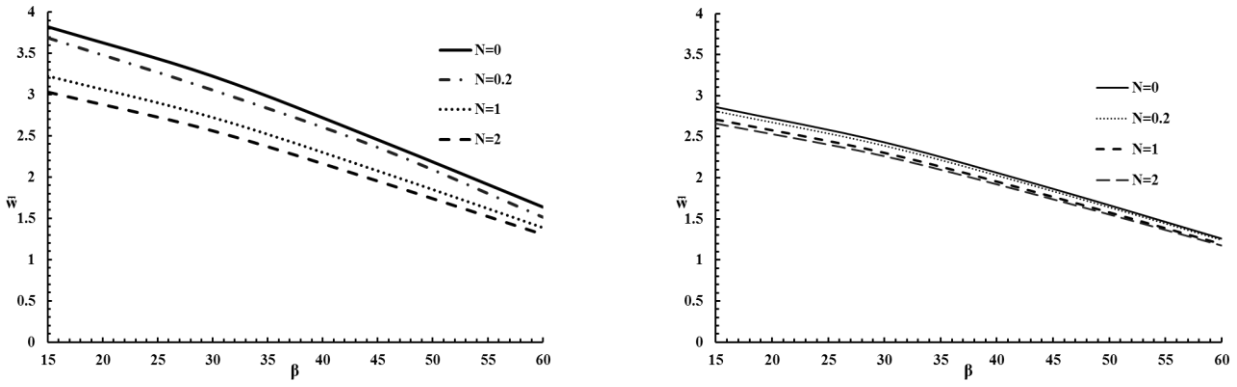

(a) 2-1-2 conical sandwich shells (b) 1-8-1 conical sandwich shells

Fig. 5 Variation of the fundamental frequency with semi vertex angle

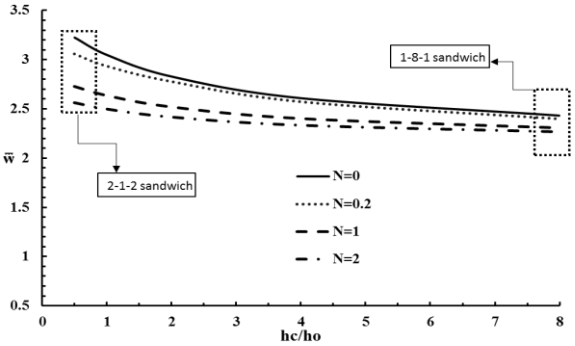

Fig. 6 Variation of the fundamental frequency with core to face sheet thickness ratio for different power law indices

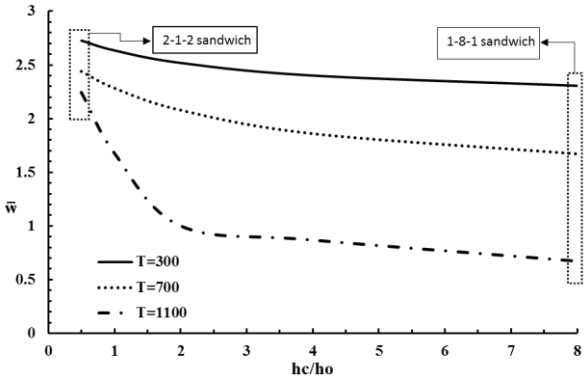

Fig. 7 Variation of the fundamental frequency with core to face sheet thickness ratio for different temperature (N = 1)

mental frequency parameter of 2-1-2 sandwich is more than 1-8-1, but for high power law indices with higher ratios, the values of two types of sandwiches are close to each other.

Fig. 6 depicts variation of the core to face sheet thickness ratio, h_c/h_o, on the fundamental frequency parameter in various power law indices and constant total thickness. When h_c/h_o = 0.5, it means faces thickness are two times of the core thickness, so it shows the results of the 2-1-2 sandwich. And, when h_c/h_o = 8, it shows results of the 1-8-1 sandwich. For all indices, by increasing the ratio in a constant total thickness, the amount of metal increases and the structure will be softer, so the fundamental frequency parameters decrease. When the power law index is increased in a constant thickness, ceramic quantity will decrease and for all values of h_c/h_o, by increasing the ratio, the fundamental frequency parameters decrease. Also, Fig. 7 shows the changing of core to face sheet thickness ratio versus fundamental frequency parameter in different temperatures. It can be observed that increasing the ratio for all temperatures and increasing the temperature in a constant ratio causes to decreasing the fundamental frequency parameters.

In order to clearly understand the porosity influence, Figs. 8 and 9 show the even and uneven porosity distributions influence on the frequency variation with (L/h = 100, $R1/L$ = 2, $\beta = \pi/6$) for the 2-1-2 and 1-8-1 sandwich shells, respectively. As depicted in Figs. 8(a) and 9(a), it is found that in the case of 2-1-2, both porosity distributions are dependent of power law indices. By increasing the porosity volume fraction, the fundamental frequency parameter first increases at lower gradient indices, but from a certain value of the power law index, increasing porosity volume leads to decreasing the fundamental frequency parameter. These increasing and decreasing are stronger in the case of even porosity distribution. In even distributions, porosities occur all over the cross-section of FG layer, while, in uneven distribution, porosities are available at middle zone of cross section. But in 1-8-1 sandwich, with increasing the porosity volume fraction, the fundamental frequency parameters always decrease but this effect is very low.

Table 5 The fundamental frequency parameters in non-uniform temperature distributions for 2-1-2 and 1-8-1 sandwiches

	T_o (k)	The Fundamental frequency			
		300	500	700	900
2-1-2	Linear	3.224691	3.171938	3.12206	3.06727
	Non-linear	3.224691	3.189249	3.151791	3.107986
1-8-1	Linear	2.431751	2.263226	2.032871	1.459472
	Non-linear	2.431751	2.312537	2.175682	1.566189

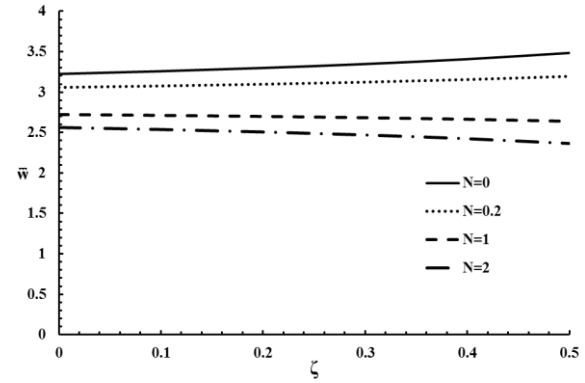

(a) 2-1-2 conical sandwich shells

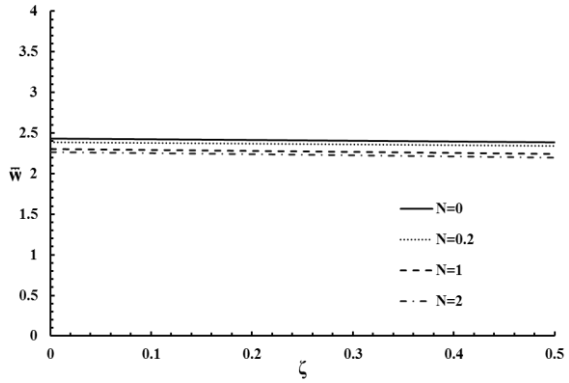

(b) 1-8-1 conical sandwich shells

Fig. 8 Variation of the fundamental frequency with even porosity distribution for different power law indices

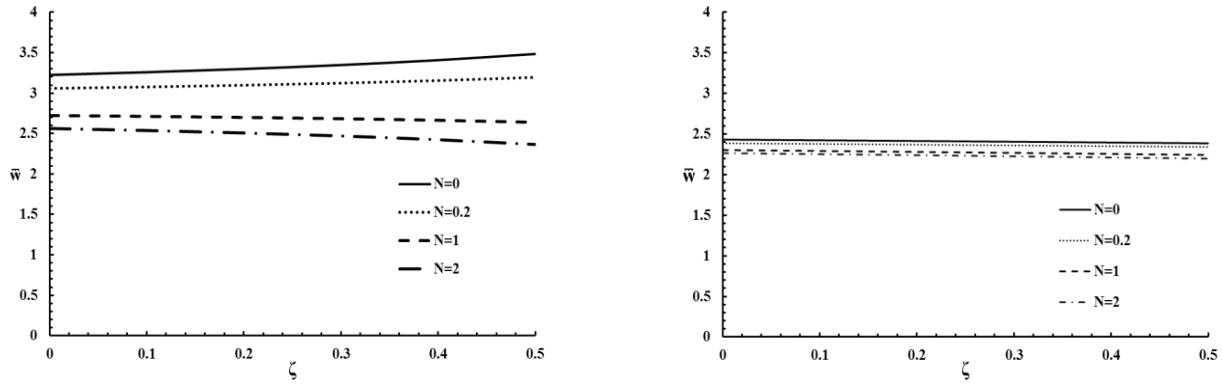

(a) 2-1-2 conical sandwich shells (b) 1-8-1 conical sandwich shells

Fig. 9 Variation of the fundamental frequency with uneven porosity distribution for different power law indices

As mentioned in section 2.2 and section 2.3, three types of temperature distributions have been considered in this paper. The uniform temperature variations have been shown in Fig. 3. In Table 5, the fundamental frequency parameters in the linear and nonlinear temperature distributions are depicted for a 2-1-2 and 1-8-1 FG truncated sandwich shells. The temperature of inner surface of sandwiches, Ti, is constant and equal to 300 (k) and the outer surface of sandwiches, T_o, is variable. Temperature between these two surfaces changes linearly based on Eqs. (6)-(8) and nonlinearly based on Eqs. (11)-(13).

7. Conclusions

In this study for two kinds of conical sandwich shells, 2-1-2 and 1-8-1, according to a high order sandwich shell theory, the displacement fields of the face-sheets were considered based on the first order shear deformation theory and the core displacement fields were considered as the cubic distributions for vertical and horizontal deflections. High order stress and thermal stress resultants, in plane and thermal stresses were considered in the core to improve the high order theory. Nonlinear strains were used for both mechanical and thermal stresses to obtain the more accurate equations that causes the problem be more complicated.

Also, the material properties of the face-sheets and the core were considered temperature-dependent. A power law distribution with different porosity distributions was used to model the temperature dependent material properties of the FG face sheets. Uniform, linear and nonlinear temperature distributions were considered to model the effect of the temperature changing in the sandwich shell. The equations of motion were obtained by Hamilton's principal and solved by using Galerkin method. Also, an approach was used to reduce the equations of motion from 28 to 16 equations. In order to survey the capabilities of this model for free vibration analysis of simply supported truncated conical sandwich shells with porous FG face sheets, the results were verified by FEM results and in a special case by literature results. Based on the results, there was a good agreement between them and the following conclusion can be drawn:

- Increasing the temperature reduces the mechanical properties. So, with increasing the temperature in a constant power law index, the fundamental frequency parameter decreases and 1-8-1 sandwich is too weaker than 2-1-2 one in higher temperature environments.
- While power law index is increased, the amount of ceramic reduces, so the fundamental frequency parameter decreases.
- In a constant power law index and a constant temperature for both sandwiches, the fundamental frequency parameter decreases when length to thickness ratio is increased.
- With increasing the semi vertex angle, the fundamental frequency parameter decreases.
- In a constant power law index, the fundamental frequency parameter decreases when radius to thickness ratio is increased.
- In a constant total thickness, with increasing the core to face-sheet thickness ratio in different temperatures and different power law indices, the fundamental frequency parameters decrease. For example, in the value of h_c/h_o = 0.5, 2-1-2 type, FG faces sandwiches due to the more quantity of ceramic have stiffer structure than the value of h_c/h_o = 8, 1-8-1 type, so the fundamental frequency parameter in 2-1-2 type is higher.
- In 2-1-2 sandwich, in the lower power law indices, with increasing the porosity volume fraction, the fundamental frequency parameter increases, but with increasing the power law index, this becomes vice versa and the fundamental frequency parameter decreases. These increasing and decreasing are more in the case of even porosity distribution. But in 1-8-1 sandwich, with increasing the porosity volume fraction, the fundamental frequency parameters always decrease.
- Frequencies in the case of non-linear distribution of temperature are bigger than the linear one.

References

Akbas, S.D. (2017), "Post-buckling responses of functionally graded beams with porosities", *Steel Compos. Struct., Int. J.*, **24**(5), 579-589. http://dx.doi.org/10.12989/scs.2017.24.5.579

Arioui, O., Belakhdar, K., Kaci, A. and Tounsi, A. (2018), "Thermal buckling of FGM beams having parabolic thickness variation and temperature dependent materials", *Steel Compos. Struct., Int. J.*, **27**(6), 777-788. http://dx.doi.org/10.12989/scs.2018.27.6.777

Atmane, H.A., Tounsi, A., Bernard, F. and Mahmoud, S.R. (2015), "A computational shear displacement model for vibrational analysis of functionally graded beams with porosities", *Steel Compos. Struct., Int. J.*, **19**(2), 369-384. http://dx.doi.org/10.12989/scs.2015.19.2.369

Bardell, N.S., Langley, R.S., Dunsdon, J.M. and Aglietti, G.S. (1999), "An h–p finite element vibration analysis of open conical sandwich panels and conical sandwich frusta", *J. Sound Vib.*, **226**(2), 345-377. https://doi.org/10.1006/jsvi.1999.2301

Barka, M., Benrahou, K.H., Bakora, A. and Tounsi, A. (2016), "Thermal post-buckling behavior of imperfect temperature-dependent sandwich FGM plates resting on Pasternak elastic foundation", *Steel Compos. Struct., Int. J.*, **22**(1), 91-112. http://dx.doi.org/10.12989/scs.2016.22.1.091

Benferhat, R., Hassaine, D., Hadji, L. and Said, M. (2016), "Static analysis of the FGM plate with porosities", *Steel Compos. Struct., Int. J.*, **21**(1), 123-136. http://dx.doi.org/10.12989/scs.2016.21.1.123

Benlahcen, F., Belakhdar, K., Sellami, M. and Tounsi, A. (2018), "Thermal buckling resistance of simply supported FGM plates with parabolic-concave thickness variation", *Steel Compos. Struct., Int. J.*, **29**(5), 591-602. http://dx.doi.org/10.12989/scs.2018.29.5.591

Bouderba, B. (2018), "Bending of FGM rectangular plates resting on non-uniform elastic foundations in thermal environment using an accurate theory", *Steel Compos. Struct., Int. J.*, **27**(3), 311-325. http://dx.doi.org/10.12989/scs.2018.27.3.311

Boutahar, L. and Benamar, R. (2016), "A homogenization procedure for geometrically non-linear free vibration analysis of functionally graded annular plates with porosities, resting on elastic foundations", *Ain Shams Eng. J.*, **7**(1), 313-333. https://doi.org/10.1016/j.asej.2015.11.016

Chen, C.S., Liu, F.H. and Chen, W.R. (2017), "Vibration and stability of initially stressed sandwich plates with FGM face sheets in thermal environments", *Steel Compos. Struct., Int. J.*, **23**(3), 251-261. http://dx.doi.org/10.12989/scs.2017.23.3.251

Dehkordi, M.B. and Khalili, S.M.R. (2015), "Frequency analysis of sandwich plate with active SMA hybrid composite face-sheets and temperature dependent flexible core", *Compos. Struct.*, **123**, 408-419. https://doi.org/10.1016/j.compstruct.2014.12.068

Fard, K.M. (2015), "Higher order static analysis of truncated conical sandwich panels with flexible cores", *Steel Compos. Struct., Int. J.*, **19**(6), 1333-1354. http://dx.doi.org/10.12989/scs.2015.19.6.1333

Fazzolari, F.A. (2015), "Natural frequencies and critical temperatures of functionally graded sandwich plates subjected to uniform and non-uniform temperature distributions", *Compos. Struct.*, **121**, 197-210. https://doi.org/10.1016/j.compstruct.2014.10.039

Frostig, Y., Baruch, M., Vilnay, O. and Sheinman, I. (1992), "High-order theory for sandwich-beam behavior with transversely flexible core", *J. Eng. Mech.*, **118**(5), 1026-1043. https://doi.org/10.1061/(ASCE)0733-9399(1992)118:5(1026)

Frostig, Y., Birman, V. and Kardomateas, G.A. (2018), "Non-linear wrinkling of a sandwich panel with functionally graded core–Extended high-order approach", *Int. J. Solids Struct.*, **148**, 122-139. https://doi.org/10.1016/j.ijsolstr.2018.02.023

Heydarpour, Y., Aghdam, M.M. and Malekzadeh, P. (2014), "Free vibration analysis of rotating functionally graded carbon nanotube-reinforced composite truncated conical shells", *Compos. Struct.*, **117**, 187-200. https://doi.org/10.1016/j.compstruct.2014.06.023

Jin, G., Ye, T. and Su, Z. (2015), "Conical Shells", In: *Structural Vibration*, Springer, Berlin, Heidelberg, Germany.

Kettaf, F.Z., Houari, M.S.A., Benguediab, M. and Tounsi, A. (2013), "Thermal buckling of functionally graded sandwich plates using a new hyperbolic shear displacement model", *Steel Compos. Struct., Int. J.*, **15**(4), 399-423. http://dx.doi.org/10.12989/scs.2013.15.4.399

Khalili, S.M.R. and Mohammadi, Y. (2012), "Free vibration analysis of sandwich plates with functionally graded face sheets and temperature-dependent material properties: A new approach", *Eur. J. Mech. A-Solid*, **35**, 61-74. https://doi.org/10.1016/j.euromechsol.2012.01.003

Khayat, M., Dehghan, S.M., Najafgholipour, M.A. and Baghlani, A. (2018), "Free vibration analysis of functionally graded cylindrical shells with different shell theories using semi-analytical method", *Steel Compos. Struct., Int. J.*, **28**(6), 735-748. http://dx.doi.org/10.12989/scs.2018.28.6.735

Kiani, Y., Dimitri, R. and Tornabene, F. (2018), "Free vibration study of composite conical panels reinforced with FG-CNTs", *Eng. Struct.*, **172**, 472-482. https://doi.org/10.1016/j.engstruct.2018.06.006

Li, F.M., Kishimoto, K. and Huang, W.H. (2009), "The calculations of natural frequencies and forced vibration responses of conical shell using the Rayleigh–Ritz method", *Mech. Res. Commun.*, **36**(5), 595-602. https://doi.org/10.1016/j.mechrescom.2009.02.003

Liu, R.H. and Li, J. (1995), "Non-linear vibration of shallow conical sandwich shells", *Int. J. Nonlin. Mech.*, **30**(2), 97-109. https://doi.org/10.1016/0020-7462(94)00032-6

Liu, M., Cheng, Y. and Liu, J. (2015), "High-order free vibration analysis of sandwich plates with both functionally graded face sheets and functionally graded flexible core", *Compos. Part B-Eng.*, **72**, 97-107. https://doi.org/10.1016/j.compositesb.2014.11.037

Mahamood, R.M. and Akinlabi, E.T. (2017), "Types of Functionally Graded Materials and Their Areas of Application", In: *Functionally Graded Materials*. Topics in Mining, Metallurgy and Materials Engineering, Springer, Cham.

Malekzadeh, P., Fiouzb, A.R. and Sobhrouyan, M. (2012), "Three-dimensional free vibration of functionally graded truncated conical shells subjected to thermal environment", *Int. J. Pres. Ves. Pip.*, **89**, 210-221. https://doi.org/10.1016/j.ijpvp.2011.11.005

Menasria, A., Bouhadra, A., Tounsi, A., Bousahla, A.A. and Mahmoud, S.R. (2017), "A new and simple HSDT for thermal stability analysis of FG sandwich plates", *Steel Compos. Struct., Int. J.*, **25**(2), 157-175. https://doi.org/10.12989/scs.2017.25.2.157

Mouli, B.C., Kar, V.R., Ramji, K. and Rajesh, M. (2018), "Free vibration of functionally graded conical shell", *Mater. Today-Proc.*, **5**(6), 14302-14308. https://doi.org/10.1016/j.matpr.2018.03.012

Najafov, A.M., Sofiyev, A.H. and Kuruoglu, N. (2014), "On the solution of nonlinear vibration of truncated conical shells covered by functionally graded coatings", *Acta Mech.*, **225**(2), 563-580. https://doi.org/10.1007/s00707-013-0980-5

Reddy, J.N. (1998), "Thermo Mechanical Behavior of Functionally Graded Materials", Texas A&M University GE Station Department of Mechanical Engineering.

Reddy, J.N. (2000), "Analysis of functionally graded plates", *Int. J. Numer. Meth. Eng.*, **47**(1-3), 663-684. https://doi.org/10.1002/(SICI)1097-0207(20000110/30)47:1/3<663::AID-NME787>3.0.CO;2-8

Reddy J.N. (2003), *Mechanics of Laminated Composite Plates and Shells, Theory and Application*, CRC Press, New York, USA.

Reddy, J.N. (2007), *Theory and Analysis of Elastic Plates and Shells*, CRC Press, New York, USA.

Salami, S.J. and Dariushi, S. (2018), "Geometrically nonlinear analysis of sandwich beams under low velocity impact: analytical and experimental investigation", *Steel Compos. Struct., Int. J.*, **27**(3), 273-283. http://dx.doi.org/10.12989/scs.2018.27.3.273

Shakouri, M. (2019), "Free vibration analysis of functionally graded rotating conical shells in thermal environment", *Compos. Part B-Eng.*, **163**, 574-584. https://doi.org/10.1016/j.compositesb.2019.01.007

Shen, H.S. (2009), *Functionally Graded Materials Nonlinear Analysis of Plates and Shells*, CRC Press, New York, USA.

Shokravi, M. (2017), "Buckling of sandwich plates with FG-CNT-reinforced layers resting on orthotropic elastic medium using Reddy plate theory", *Steel Compos. Struct., Int. J.*, **23**(6), 623-631. http://dx.doi.org/10.12989/scs.2017.23.6.623

Shu, C. (1996), "An efficient approach for free vibration analysis of conical shells", *Int. J. Mech. Sci.*, **38**(8-9), 935-949. https://doi.org/10.1016/0020-7403(95)00096-8

Sofiyev, A.H. (2012), "The non-linear vibration of FGM truncated conical shells", *Compos. Struct.*, **94**(7), 2237-2245. https://doi.org/10.1016/j.compstruct.2012.02.005

Sofiyev, A.H. (2015), "Buckling analysis of freely-supported functionally graded truncated conical shells under external pressures", *Compos. Struct.*, **132**, 746-758. https://doi.org/10.1016/j.compstruct.2015.06.026

Sofiyev, A.H. (2016), "Parametric vibration of FGM conical shells under periodic lateral pressure within the shear deformation theory", *Compos. Part B-Eng.*, **89**, 282-294. https://doi.org/10.1016/j.compositesb.2015.11.017

Sofiyev, A.H. (2018), "Application of the first order shear deformation theory to the solution of free vibration problem for laminated conical shells", *Compos. Struct.*, **188**, 340-346. https://doi.org/10.1016/j.compstruct.2018.01.016

Sofiyev, A.H. (2019), "Review of research on the vibration and buckling of the FGM conical shells", *Compos. Struct.*, **211**, 301-317. https://doi.org/10.1016/j.compstruct.2018.12.047

Sofiyev, A.H. and Kuruoglu, N. (2015), "On a problem of the vibration of functionally graded conical shells with mixed boundary conditions", *Compos. Part B-Eng.*, **70**, 122-130. https://doi.org/10.1016/j.compositesb.2014.10.047

Sofiyev, A.H. and Osmancelebioglu, E. (2017), "The free vibration of sandwich truncated conical shells containing functionally graded layers within the shear deformation theory", *Compos. Part B-Eng.*, **120**, 197-211. https://doi.org/10.1016/j.compositesb.2017.03.054

Sofiyev, A.H. and Schnack, E. (2012), "The vibration analysis of FGM truncated conical shells resting on two-parameter elastic foundations", *Mech. Adv. Mater. Struct.*, **19**(4), 241-249. https://doi.org/10.1080/15376494.2011.642934

Tahouneh, V. (2018), "3-D Vibration analysis of FG-MWCNTs/Phenolic sandwich sectorial plates", *Steel Compos. Struct., Int. J.*, **26**(5), 649-662. http://dx.doi.org/10.12989/scs.2018.26.5.649

Talebitooti, M. (2018), "Thermal effect on free vibration of ring-stiffened rotating functionally graded conical shell with clamped ends", *Mech. Adv. Mater. Struct.*, **25**(2), 155-165. https://doi.org/10.1016/j.jsv.2009.07.031

Tornabene, F., Viola, E. and Inman, D.J. (2009), "2-D differential quadrature solution for vibration analysis of functionally graded conical, cylindrical shell and annular plate structures", *J. Sound Vib.*, **328**(3), 259-290. https://doi.org/10.1016/j.jsv.2009.07.031

Van Dung, D. and Chan, D.Q. (2017), "Analytical investigation on mechanical buckling of FGM truncated conical shells reinforced by orthogonal stiffeners based on FSDT", *Compos. Struct.*, **159**, 827-841. https://doi.org/10.1016/j.compstruct.2016.10.006

Vinson, J.R. (2018), *The Behavior of Sandwich Structures of Isotropic and Composite Materials*, TECHNOMIC, Pennsylvania, USA. https://doi.org/10.1201/9780203737101

Wang Y.Q. and Zu J.W. (2017), "Vibration behaviors of functionally graded rectangular plates with porosities and moving in thermal environment", *Aerosp. Sci. Technol.*, **69**, 550-562. https://doi.org/10.1016/j.ast.2017.07.023

CC